Available online at www.sciencedirect.com
SCIENCE DIRECT®
ELSEVIER
Journal of Computational and Applied Mathematics 177 (2005) 243–267
JOURNAL OF COMPUTATIONAL AND APPLIED MATHEMATICS
www.elsevier.com/locate/cam

Stabilized finite element schemes with LBB-stable elements for incompressible flows

Tobias Gelhard[a], Gert Lube[a,*], Maxim A. Olshanskii[b,1], Jan-Hendrik Starcke[a]

[a] *Mathematics Department, University of Göttingen, D-37083, Germany*
[b] *Department of Mechanics and Mathematics, Moscow M.V. Lomonosov University, Moscow 119899, Russia*

Received 2 July 2003; received in revised form 8 April 2004

Abstract

We study stabilized FE approximations of SUPG type to the incompressible Navier–Stokes problem. Revisiting the analysis for the linearized model, we show that for conforming LBB-stable elements the design of the stabilization parameters for many practical flows differs from that commonly suggested in literature and initially designed for the case of equal-order approximation. Then we analyze a reduced SUPG scheme often used in practice for LBB-stable elements. To provide the reduced scheme with appropriate stability estimates we introduce a modified LBB condition which is proved for a family of FE approximations. The analysis is given for the linearized equations. Numerical experiments for some linear and nonlinear benchmark problems support the theoretical results.

Keywords: Finite element method; Stabilized method; LBB condition; Navier–Stokes equations

* Corresponding author. Institute of Numerical and Applied Mathematics, Georg-August-University Gottingen, Lotzestr. 16-18, Gottingen D-37083, Germany.
E-mail address: lube@math.uni-goettingen.de (G. Lube).

[1] The support of the Russian Foundation for Basic Research: grant No 03-01-06460 linked to project 02-01-00592 and the program "Russian Universities" UR.04.03.002/03 is acknowledged.

0377-0427/$ - see front matter © 2004 Elsevier B.V. All rights reserved.
doi:10.1016/j.cam.2004.09.017

1. Introduction

We consider the nonstationary incompressible Navier–Stokes problem: find a velocity $\mathbf{u}(t,\mathbf{x})$ and a kinematic pressure $p(t,\mathbf{x})$ from

$$\partial_t \mathbf{u} - \nu\Delta\mathbf{u} + (\mathbf{u}\cdot\nabla)\mathbf{u} + \nabla p = \mathbf{f}, \quad \operatorname{div}\mathbf{u} = 0 \quad \text{in } \Omega\times(0,T] \tag{1}$$

in a bounded domain $\Omega \in R^n$, $n = 2, 3$ with given force field $\mathbf{f}$ and viscosity $\nu > 0$. Boundary and initial conditions should be additionally supplied. Implicit time integration and linearization often lead to the generalized Oseen problem

$$-\nu\Delta\mathbf{u} + \alpha\mathbf{u} + (\mathbf{a}\cdot\nabla)\mathbf{u} + \nabla p = \tilde{\mathbf{f}}, \quad \operatorname{div}\mathbf{u} = g \quad \text{in } \Omega, \tag{2}$$

with a reaction term $\alpha \sim 1/\delta t$ related to the time step δt.

Finite element (FE) methods for (1) and (2) may suffer from two sources of instabilities. One is a possible incompatibility of pressure and velocity FE pairs. A remedy is a choice of FE spaces passing the inf-sup or LBB condition or the use of pressure stabilizing techniques. Another source of instabilities stems from dominating advection for large Reynolds numbers Re. There exist several variants of stabilized FE methods of arbitrary order which combine stability and accuracy, e.g. the streamline upwind/pressure stabilizing Petrov–Galerkin (SUPG/PSPG) method, the Galerkin/Least-squares (GLS) and algebraic subgrid scale (ASGS) techniques, see, e.g., [7,10,20,22,23]. These methods simultaneously suppress spurious oscillations caused by both, dominating advection and nonLBB-stable FE spaces. In particular, the popular equal-order velocity-pressure approximation is allowed.

At the same time the combination of LBB-stable velocity-pressure FE pairs with stabilization is often used in practice, see e.g. [21,23]. However it is rarely considered in numerical analysis. The goal of the present paper is to extend the analysis of [17] for conforming LBB-stable FE pairs and to provide numerical results. Below we comment on the main observations and results.

We start with *fully stabilized* schemes. For problem (2) it includes SUPG/PSPG and grad-div stabilization. A rather general result by Tobiska/Verfürth in [22] is applicable to this case. Under reasonable regularity assumptions on the solution (see [7,10,17,20]) the design of the stabilization parameters differs for LBB-stable elements from that of equal-order (LBB-unstable) pairs. The resulting error estimate is uniform with respect to ν and α. It shows a quasi-optimal convergence order, whereas the standard choice of parameters (optimal for equal-order pairs) leads to an order reduction of $\frac{1}{2}$.

For convenience we include here the analysis which simplifies the proofs in [22] and slightly improves results for conforming LBB-stable elements. The analysis does not exploit any specific information about ν-dependence of the solution. Our numerical results perfectly match the theoretical predictions for smooth, ν-independent solutions. Moreover, numerical experiments on quasi-uniform meshes with several typical flow problems (2) and (1) with ν-dependent solutions are performed to verify conclusions for more practical situations.

A natural question is whether pressure stabilization is necessary for LBB-stable FE pairs. So we consider the SUPG scheme without PSPG stabilization. This *reduced* scheme produces less additional terms; it is often used by practitioners. In our numerical experiments we found almost identical results for the reduced and the fully stabilized schemes. However a convincing numerical analysis for the reduced scheme is missing. The analysis in [17] follows the same framework of fully stabilized methods but gives unsatisfactory stability estimates. Here we improve the analysis using a *modified* inf-sup (LBB) condition, cf. Lemma 4.1. This condition was known for the simplest Taylor–Hood element, see [2]. We

extend the result to a family of LBB-stable elements with additional assumption on domain regularity and for quasi-uniform meshes. This result allows to prove uniform stability and robust error estimates for the reduced SUPG scheme if $\nu + \alpha h^2 \gtrsim h^2$ (cf. condition (28)). If this condition fails to be true, then a robust convergence analysis for this scheme is still an open problem. Numerical experiments indicate robustness of the proposed scheme for this case as well.

Problem (2) appears as auxiliary problem within an implicit time integration of the unsteady Navier–Stokes equations (1). This approach is also feasible for a problem with a stationary solution. In experiments we apply it to solve typical benchmark problems (driven cavity, backward facing step). These results indicate that the approach to the linear case remains meaningful in the nonlinear case too. The case of time-accurate solution of (1) will be considered elsewhere; see also elaborations for a stabilized equal-order method in the recent paper [9].

The remainder of the paper is organized as follows: Section 2 presents various FE schemes for the linearized equations. Section 3 is devoted to the case of fully stabilized schemes with LBB-stable pairs. The analysis for reduced stabilized schemes is then presented in Section 4. Numerical results for the linearized and nonlinear problems are given in Sections 5 and 6.

2. Stabilized FEM for the linearized model

We start with a variational formulation of (2) assuming homogeneous Dirichlet boundary conditions for $\mathbf{u}$. Set $\mathbf{V} := H_0^1(\Omega)^n$ and $Q := L_0^2(\Omega)$. A variational formulation of (2) reads: given $\mathbf{f} \in H^{-1}(\Omega)$, $g \in Q$, find $U := \{\mathbf{u}, p\} \in \mathbf{W} := \mathbf{V} \times Q$ such that

$$a(U, V) = f(V) \quad \forall V := \{\mathbf{v}, q\} \in \mathbf{W}, \tag{3}$$

$$a(U, V) := \nu(\nabla\mathbf{u}, \nabla\mathbf{v}) + (\alpha\mathbf{u} + (\mathbf{a}\cdot\nabla)\mathbf{u}, \mathbf{v}) - (p, \operatorname{div}\mathbf{v}) + (q, \operatorname{div}\mathbf{u}),$$

$$f(V) := \langle\mathbf{f}, \mathbf{v}\rangle + (g, q).$$

Remark. Additionally we assume $\mathbf{a} \in L^\infty(\Omega)^n \cap H_0^1(\Omega)^n$, $\operatorname{div}\mathbf{a} = 0$. In the context of linearization of the Navier–Stokes problem the smoothness assumptions are reasonable if $\mathbf{a}$ is a FE velocity field. The second condition ensures that $((\mathbf{a}\cdot\nabla)\mathbf{u}, \mathbf{v})$ is skew-symmetric. For FE functions this condition is usually valid in a weak sense only and the skew-symmetry of the bilinear form can be lost. The simplest way is to use the skew-symmetric form $\frac{1}{2}((\mathbf{a}\cdot\nabla)\mathbf{u}, \mathbf{v}) - \frac{1}{2}((\mathbf{a}\cdot\nabla)\mathbf{v}, \mathbf{u})$. This modification does not alter our analysis.

Let $\mathscr{T}_h := \{K\}$ be a regular family of simplicial triangulations of $\bar{\Omega}$. We denote by h_K and ρ_K the diameter of the minimal ball circumscribed on an element K, respectively the maximal ball inscribed in K. Suppose that $\mathscr{T}_h$ is shape-regular such that $h_K/\rho_K \leqslant c$ for all K with constant $c \neq c(h)$. This condition allows local mesh refinement but excludes an anisotropic refinement of layers. Assume that an $\mathscr{T}_h$ is an exact triangulation of $\bar{\Omega}$. For any element $\tau \in \mathscr{T}_h$ the local inner product in $L^2(\tau)$ is denoted by $(\cdot,\cdot)_\tau$. For the global scalar product and norm in $L^2(\Omega)$ we simply write $(\cdot,\cdot)$ and $\|\cdot\|$.

Let $\mathbf{V}_h \subset \mathbf{V}$ and $Q_h \subset Q$ be conforming FE spaces to approximate velocity and pressure, consisting of piecewise polynomials of degree $l = 1, 2, \ldots$ and $k = 0, 1, \ldots$. Later on we use local inverse

inequalities [4] on $\mathbf{V}_h$ and Q_h for all elements $\tau \in \mathcal{T}_h$:

$$\|\Delta \mathbf{v}_h\|_\tau \leqslant \mu_u h_\tau^{-1} \|\nabla \mathbf{v}_h\|_\tau, \quad \|\nabla v_h\|_\tau \leqslant \mu_u h_\tau^{-1} \|v_h\|_\tau, \quad \|\nabla q_h\|_\tau \leqslant \mu_p h_\tau^{-1} \|q_h\|_\tau. \tag{4}$$

The basic Galerkin finite element method for (3) reads: find $U_h = \{\mathbf{u}_h, p_h\} \in \mathbf{W}_h = \mathbf{V}_h \times Q_h$ such that

$$a(U_h, V_h) = f(V_h) \quad \forall V_h = \{\mathbf{v}_h, q_h\} \in \mathbf{W}_h. \tag{5}$$

We consider velocity/pressure approximations $\mathbf{V}_h \times Q_h$, which are *LBB-stable*, i.e. the following Ladyzhenskaya–Babuška–Brezzi condition is valid: there exists a positive h-independent constant β_0 such that

$$\inf_{q_h \in Q_h} \sup_{\mathbf{V}_h \in \mathbf{V}_h} \frac{(q_h, \operatorname{div} \mathbf{v}_h)}{\|\nabla \mathbf{v}_h\| \, \|q_h\|} \geqslant \beta_0. \tag{6}$$

Henceforth $\sup_x$ and $\inf_x$ are taken for $x \neq 0$ if $\|x\|$ appears in the denominator. Typical examples are the P_{k+1}/P_k elements of the Taylor–Hood family with $k \geqslant 1$ which will be used in Sections 5–6.

The Galerkin scheme (5) may exhibit spurious solutions if the mesh is too coarse in order to resolve instabilities stemming from locally dominating advection, i.e. the mesh Reynolds numbers $\mathrm{Re}_\tau = \|\mathbf{a}\|_{\infty,\tau} h_\tau \nu^{-1}$ are large. This can be seen even for solutions without sharp layers and very small values of $\nu > 0$.

The standard stabilization methods for problem (3) are of the following type: find $U_h = \{\mathbf{u}_h, p_h\} \in \mathbf{W}_h$ such that

$$a_h(U_h, V_h) = f_h(V_h) \quad \forall V_h = \{\mathbf{v}_h, q_h\} \in \mathbf{W}_h, \tag{7}$$

$$a_h(U, V) := a(U, V) + \sum_\tau (\gamma_\tau \operatorname{div} \mathbf{u}, \operatorname{div} \mathbf{v})_\tau + \sum_\tau (\mathcal{L}(U), \delta_\tau \psi(V))_\tau, \tag{8}$$

$$f_h(V) := f(V) + \sum_\tau ((\gamma_\tau g, \operatorname{div} \mathbf{v})_\tau + (\mathbf{f}, \delta_\tau \psi(V))_\tau). \tag{9}$$

Here $\mathcal{L}$ denotes the differential operator on the left-hand side of momentum equation in (2). We shall comment on a choice of $\psi(V)$ below. Constants δ_τ and γ_τ are some stabilization parameters, in general they can be problem dependent.

The stabilized scheme (7)–(9) is built of residual type, i.e. the sum of additional terms vanishes for a smooth solution of (2). This implies the Galerkin orthogonality

$$a_h(U - U_h, V_h) = 0 \quad \forall V_h \in \mathbf{W}_h. \tag{10}$$

The Galerkin scheme (5) is a special case of (7) with $\gamma_\tau = \delta_\tau = 0$. Another special case $\delta_\tau = 0$, $\gamma_\tau > 0$ will be called grad-div stabilization since, for a constant set $\gamma_\tau = \gamma$, the corresponding term acts as an additional term $-\gamma \nabla \operatorname{div} \mathbf{u}$ in (2).

3. Fully stabilized schemes with LBB-stable elements

In this section we consider the scheme (7)–(9) with

$$\psi(V) = (\mathbf{a} \cdot \nabla)\mathbf{v} + \nabla q.$$

This choice can also be found in [6,10,17,20,22]. Other possible ("expensive") variants are the GLS method with $\psi(V) = \mathscr{L}(V)$ and the Douglas–Wang or algebraic subgrid-scale methods with $\psi(V) = -\mathscr{L}^*(V)$ with the adjoint operator $\mathscr{L}^*$, cf. [7]. These methods can be analyzed using the norm

$$|||V|||_a := (|[V]|_a^2 + \sigma_a \|q\|^2)^{1/2}, \tag{11}$$

$$|[V]|_a^2 = \nu\|\nabla \mathbf{v}\|^2 + \alpha\|\mathbf{v}\|^2 + \sum_\tau (\gamma_\tau \|\operatorname{div} \mathbf{v}\|_\tau^2 + \delta_\tau \|(\mathbf{a}\cdot\nabla)\mathbf{v} + \nabla q\|_\tau^2). \tag{12}$$

Gaining additional control of $\sum_\tau \delta_\tau \|(\mathbf{a}\cdot\nabla)\mathbf{u} + \nabla p\|_\tau^2$ and of the incompressibility constraint, these methods simultaneously stabilize spurious Galerkin solutions coming from dominating advection and violation of the discrete LBB-condition. Therefore we call them *fully stabilized* methods. In particular, they allow (not LBB-stable) equal-order approximation $l = k \geqslant 1$ of velocity and pressure [10].

The rather general result in [22], Section 3 covers the analysis of scheme (7)–(9) with $\psi(V) = (\mathbf{a}\cdot\nabla)\mathbf{v} + \nabla q$ in the case of LBB-stable elements where typically $l \geqslant k+1 \geqslant 1$. For convenience we include here the analysis which simplifies the proofs in [22] and slightly improves results. We start with a stability result.

Lemma 3.1. *Assume the following condition on stabilization parameters*

$$0 \leqslant \delta_\tau \leqslant \frac{1}{2}\min\left\{\frac{h_\tau^2}{\mu_u^2 \nu}, \frac{1}{\alpha}\right\}, \quad 0 \leqslant \delta_\tau \mathbf{a}_\tau^2 \leqslant \gamma_\tau, \tag{13}$$

with $\mathbf{a}_\tau := \|\mathbf{a}\|_{L^\infty(\tau)}$. *Then there exists a positive constant* $\beta_a \neq \beta_a(h,\nu)$ *such that the bilinear form* $a_h(\cdot,\cdot)$ *defined in* (7)–(9) *satisfies*

$$\inf_{U_h \in \mathbf{W}_h} \sup_{V_h \in \mathbf{W}_h} \frac{a_h(U_h, V_h)}{|||U_h|||_a |||V_h|||_a} \geqslant \beta_a. \tag{14}$$

Parameter σ_a in Eq. (11) can be taken as

$$\sqrt{\sigma_a} = c\left(\sqrt{\gamma} + \sqrt{\nu} + \sqrt{\alpha}C_F + \frac{C_F\|\mathbf{a}\|_\infty}{\sqrt{\nu + \alpha C_F^2}}\right)^{-1}. \tag{15}$$

Proof. Given in the Appendix. □

Remark. A simplified analysis is possible using the fact that $|[\cdot]|_a$ is a mesh-dependent norm on $\mathbf{W}_h$. For arbitrary $U_h \in \mathbf{W}_h$ we obtain $a_h(U_h, U_h) \geqslant \frac{1}{2}|[U_h]|_a^2$; this already yields existence of the discrete solution. □

The following continuity result reflects the effect of stabilization: The L^2-terms on the right-hand side of (16) explode for $\nu, \alpha \to 0$ if $\gamma_\tau = 0$.

Lemma 3.2. *In addition to the assumptions of Lemma* 3.1 *let* $\delta_\tau > 0$. *Then for each* $U = \{\mathbf{u}, p\} \in \mathbf{W}$ *with* $\Delta\mathbf{u}|_\tau \in L^2(\tau)^n \ \forall \tau \in \mathscr{T}_h$ *and* $V_h = \{\mathbf{v}_h, q_h\} \in \mathbf{W}_h$ *it holds*

$$\frac{a_h(U, V_h)}{|||V_h|||_a} \leqslant C \left\{ |[U]|_a + \left(\sum_\tau (\delta_\tau)^{-1} \|\mathbf{u}\|_\tau^2 \right)^{1/2} + \left(\sum_\tau \frac{2}{\nu + \gamma_\tau} \|p\|_\tau^2 \right)^{1/2} + \left(\sum_\tau \delta_\tau \| - \nu\Delta\mathbf{u} + \alpha\mathbf{u}\|_\tau^2 \right)^{1/2} \right\}. \tag{16}$$

Proof. The symmetric terms of a_h are bounded by the product $|[U]|_a |[V_h]|_a$. Furthermore, using integration by parts, we get

$$((\mathbf{a} \cdot \nabla)\mathbf{u}, \mathbf{v}_h) + (\operatorname{div} \mathbf{u}, q_h) \leqslant \left(\sum_\tau (\delta_\tau)^{-1} \|\mathbf{u}\|_\tau^2 \right)^{1/2} \left(\sum_\tau \delta_\tau \|(\mathbf{a} \cdot \nabla)\mathbf{v}_h + \nabla q_h\|_\tau^2 \right)^{1/2},$$

$$-(p, \operatorname{div} \mathbf{v}_h) \leqslant \left(\sum_\tau \frac{2}{\nu + \gamma_\tau} \|p\|_\tau^2 \right)^{1/2} \left(\nu \|\nabla \mathbf{v}_h\|^2 + \sum_\tau \gamma_\tau \|\operatorname{div} \mathbf{v}_h\|_\tau^2 \right)^{1/2}.$$

For the remaining terms it holds

$$\sum_\tau \delta_\tau (-\nu\Delta\mathbf{u} + \alpha\mathbf{u}, (\mathbf{a} \cdot \nabla)\mathbf{v}_h + \nabla q_h)_\tau \leqslant \left(\sum_\tau \delta_\tau \| - \nu\Delta\mathbf{u} + \alpha\mathbf{u}\|_\tau^2 \right)^{1/2} \left(\sum_\tau \delta_\tau \|(\mathbf{a} \cdot \nabla)\mathbf{v}_h + \nabla q_h\|_\tau^2 \right)^{1/2}.$$

This implies the assertion (16) via the definition of $|||\cdot|||_a$ and $|[\cdot]|_a$. □

Consider solutions $\{\mathbf{u}, p\} \in \mathbf{W}$ and $\{\mathbf{u}_h, p_h\} \in \mathbf{W}_h$ of the continuous and of the discrete problems, respectively. The following error estimate for $E_h = \{\mathbf{u} - \mathbf{u}_h, p - p_h\}$ differs from the standard result for equal-order FE pairs.

Theorem 3.1. *Assume such scaling of* (2) *that* $\|\mathbf{a}\|_\infty = \mathrm{O}(1)$. *The fully stabilized scheme* (7)–(9) *with parameters*

$$\gamma_\tau = \gamma \sim 1, \quad \delta_\tau \sim h_\tau^2/\gamma, \tag{17}$$

satisfying (13) *and with LBB-stable elements with* $l \geqslant k + 1$, *obeys the uniform error estimate*

$$|||E_h|||_a^2 \leqslant C \sum_\tau \{h_\tau^{2(k+1)} |p|_{H^{k+1}(\tau)}^2 + h_\tau^{2l} |\mathbf{u}|_{H^{l+1}(\tau)}^2\}, \quad C \neq C(\nu, \alpha, h). \tag{18}$$

Proof. Let $\{\hat{\mathbf{u}}_h, \hat{p}_h\} \in \mathbf{W}_h$ be an appropriate interpolant for $\{\mathbf{u}, p\}$. Consider

$$\{\eta_\mathbf{u}, \eta_p\} := \{\mathbf{u} - \hat{\mathbf{u}}_h, p - \hat{p}_h\}, \quad \{\chi_\mathbf{u}, \chi_p\} := \{\hat{\mathbf{u}}_h - \mathbf{u}_h, \hat{p}_h - p_h\}.$$

Galerkin orthogonality (10) and (14) imply that there exists $V_h \in \mathbf{W}_h$ with

$$\beta_a |||\{\chi_{\mathbf{u}}, \chi_p\}|||_a |||V_h|||_a \leqslant a_h(\{\chi_{\mathbf{u}}, \chi_p\}, V_h) = -a_h(\{\eta_{\mathbf{u}}, \eta_p\}, V_h). \tag{19}$$

We combine (19) and Lemma 3.2 with $U = \{\eta_{\mathbf{u}}, \eta_p\}$ to get

$$\beta_a |||\{\chi_{\mathbf{u}}, \chi_p\}|||_a \leqslant |[\{\eta_{\mathbf{u}}, \eta_p\}]|_a + \left(\sum_\tau \delta_\tau \| - \nu\Delta\eta_{\mathbf{u}} + \alpha\eta_{\mathbf{u}}\|_\tau^2\right)^{1/2} + \left(\sum_\tau \frac{2}{\nu + \gamma_\tau}\|\eta_p\|_\tau^2\right)^{1/2} + \left(\sum_\tau \delta_\tau^{-1}\|\eta_{\mathbf{u}}\|_\tau^2\right)^{1/2}.$$

Then the triangle inequality $|||E_h|||_a \leqslant |||\{\chi_{\mathbf{u}}, \chi_p\}|||_a + |||\{\eta_{\mathbf{u}}, \eta_p\}|||_a$ and standard local interpolation properties together with assumption (13) imply that

$$|||E_h|||_a^2 \leqslant C \sum_\tau \left\{ (\delta_\tau + h_\tau^2(\nu + \gamma_\tau)^{-1} + \sigma_a h_\tau^2) h_\tau^{2k} |p|_{H^{k+1}(\tau)}^2 + \left(\nu + \alpha C_F^2 h_\tau^2 + \gamma_\tau + \delta_\tau\left(\mathbf{a}_\tau^2 + \frac{\nu^2}{h_\tau^2} + \alpha^2 h_\tau^2\right) + \frac{h_\tau^2}{\delta_\tau}\right) h_\tau^{2l} |\mathbf{u}|_{H^{l+1}(\tau)}^2 \right\}. \tag{20}$$

For LBB-stable elements with $l \geqslant k+1$ a reasonable balance of the right-hand side terms gives the choice $\gamma_\tau = \gamma \sim 1$, $\delta_\tau \sim h_\tau^2/\gamma$. The estimate (20) yields

$$|||E_h|||_a^2 \leqslant C \sum_\tau \{(1 + \sigma_a) h_\tau^{2(k+1)} |p|_{H^{k+1}(\tau)}^2 + (\nu + \alpha h_\tau^2 + \gamma + h_\tau^2 \mathbf{a}_\tau^2) h_\tau^{2l} |\mathbf{u}|_{H^{l+1}(\tau)}^2\}.$$

Observing that σ_a remains bounded for ν and α (provided that $\|\mathbf{a}\|_\infty \sim 1$), and for sufficiently small h we arrive at (18). □

In the case of $\mathbf{u} \in H^{l+1}(\Omega)^n$ and $p \in H^{k+1}(\Omega)$ several conclusions of Theorem 3.1 follow, which will be confirmed by the numerical experiments in Section 5.

One is that the constant C in the error estimate (18) is uniform for arbitrary (ν, α); of course, the seminorms of the solution on the right-hand side can depend on (ν, α). With a fixed ν and α the estimate gives optimal convergence order in terms of k and l, see Experiments 5.1 and 5.2 in Section 5. Similar results can be found in [22], Remark 3.4 and [20], Remark IV.3.6, but here we improved constant σ_a.

Let us compare (18) with the error estimate for the *unstabilized* Galerkin scheme with LBB-stable elements. In the interesting case of $\|\mathbf{a}\|_\infty \sim 1$, $\nu \leqslant h$ our analysis gives the following error estimate

$$\|E_h\|_g^2 \leqslant C \sum_\tau \frac{1}{\nu + \alpha h_\tau^2} \{h_\tau^{2(k+1)} |p|_{H^{k+1}(\tau)}^2 + h_\tau^{2(l+1)} |\mathbf{u}|_{H^{l+1}(\tau)}^2\} \tag{21}$$

with $\|\{\mathbf{v}, q\}\|_g^2 := \nu\|\nabla\mathbf{v}\|^2 + \alpha\|\mathbf{v}\|^2 + \sigma_g\|q\|^2$ and $\sigma_b \sim \nu + \alpha C_F^2$. Note that for the unstabilized method the error is controlled in a weaker norm ($\|E_h\|_g \leqslant |||E_h|||_a$). Moreover the main effect of stabilization is that the factor $\frac{1}{\nu + \alpha h_\tau^2}$ presented in the right-hand side of (21) disappears.

The parameter design (17) for LBB-stable elements is simpler than the corresponding choice for *equal-order* interpolation:

$$\bar{\delta}_\tau = \frac{\delta_0 h_\tau^2}{\nu(1+\mathrm{Re}_\tau + D_\tau)}, \quad \tilde{\gamma}_\tau = \gamma_0 \nu(1+\mathrm{Re}_\tau + D_\tau) \tag{22}$$

with $D_\tau = \alpha h_\tau^2 \nu^{-1}$. Relations (22) can be derived from (20) for $l = k \geqslant 1$. For equal-order elements it provides a convergence order of $\mathcal{O}(h^{k+\frac{1}{2}})$ with respect to the norm $|[\cdot]|_a$ in the advection-dominated case $\mathrm{Re}_\tau \geqslant 1$, see [7,10,17,22].

Moreover, the use of (22) for FE pairs with $l \geqslant k+1$ also gives a convergence order of $\mathcal{O}(h^{k+\frac{1}{2}})$ with respect to the $|||\cdot|||_a$-norm. Comparing to (18), one notes an order reduction of $\frac{1}{2}$. This will be confirmed in Experiments 5.1-2 in Section 5.

We remark that for elements with $l \geqslant k+1$ the role of grad-div stabilization becomes more important. It suppresses one more possible source of instability caused by a large pressure gradient in the momentum equations in (2). The choice of $\gamma_\tau \sim 1$ minimizes the pressure-dependent term on the right-hand side of the error estimate. The main effect is seen in improving the velocity approximation, cf. also [19] and Experiment 5.2 in Section 5.

So far no specific ν-dependence of $(\mathbf{u}, p)$ is assumed. An existing regularity theory for the Navier–Stokes problem conjectures that the norms $\|\mathbf{u}\|_{l+1}$ and $\|p\|_l$ are of comparable size. If this is the case, then element pairs with $l > k+1$ are more appropriate than equal-order pairs with $l = k$. See also Experiment 5.1.

Finally, results of the section as well as those found in other papers demonstrate that fully stabilized methods admit transparent numerical analysis. Nevertheless some critical comments are also found in literature:

- The parameter design (22) for equal-order pairs is sensitive to the particular choice of constants δ_0, γ_0. A wrong choice can lead to over- or under-stabilization [23]. On the other hand, from numerical experiments in Section 5 we learn that the choice (17) for LBB-stable elements is less sensitive.
- The assembling of the corresponding algebraic system for these methods is very expensive, especially for $n = 3$, see, e.g., [23].
- The construction of efficient iterative solvers is complicated due to the velocity/pressure coupling in the stabilization terms, see, e.g., [16].

A few questions remain open for the fully stabilized scheme:

- The physical meaning of the term $\sum_\tau \delta_\tau \|(\mathbf{a}\cdot\nabla)\mathbf{u} + \nabla p\|_\tau^2$, by contrast with the classical SUPG term $\sum_\tau \delta_\tau \|(\mathbf{a}\cdot\nabla)\mathbf{u}\|_\tau^2$, is not clear.
- In our analysis and other papers, e.g. [22], the control of the L^2-norm of the pressure is lost for ν, $\alpha \to +0$ since σ_a tends to zero. This is not observed in the numerical experiments. It remains an open question whether the analysis can be refined.

In Section 4 we discuss a simplification of the fully stabilized scheme. The natural question is whether the PSPG terms can be omitted for LBB-stable elements.

4. Reduced stabilized schemes

In this section we consider the scheme (7)–(9) with

$$\psi(V) := (\mathbf{a}\cdot\nabla)\mathbf{v}. \tag{23}$$

As already mentioned this is a popular choice among practitioners, when LBB stable elements are used. Indeed, numerical results with Taylor–Hood elements in Sections 5 and 6 indicate that the test function $\delta_\tau\nabla q$ in $\psi(V)$ can be omitted. This leads us to

Problem (P). *Is it possible to prove for the reduced scheme uniform error estimates similar to those in Theorem* 3.1?

A positive answer to problem (P) was known for moderate values of $\alpha > 0$, cf. [17], Remark 4.2. Here we improve this result using a modified technique. The analysis will be given with respect to the norm $|||\cdot|||_b$ defined as

$$|||V|||_b^2 = |[V]|_b^2 + \sigma_b \sum_\tau \|\nabla q\|_\tau^2, \tag{24}$$

$$|[V]|_b^2 = \nu\|\nabla\mathbf{v}\|^2 + \alpha\|\mathbf{v}\|^2 + \sum_\tau(\gamma_\tau\|\operatorname{div}\mathbf{v}\|_\tau^2 + \delta_\tau\|(\mathbf{a}\cdot\nabla)\mathbf{v}\|_\tau^2). \tag{25}$$

Trying to analyze the reduced scheme in the same framework one soon finds that troubles come from the term $\sum_\tau \delta_\tau(\nabla p_h, (\mathbf{a}\cdot\nabla)\mathbf{v}_h)_\tau$. This term disappears for piecewise constant pressure ($k=0$), see [15], but does not vanish for higher order pressure approximations ($k\geqslant 1$). For the higher order approximations a modified LBB stability condition is crucial in the further analysis. Unfortunately we are able to prove this condition only under the following assumption:

$$\left(\sup_\tau h_\tau\right)\left(\inf_\tau h_\tau\right)^{-1} \leqslant c. \tag{26}$$

This condition excludes local mesh refinement.

Lemma 4.1. *Suppose that Ω is such that a H^2-regularity result holds for the Stokes problem* (*cf.* [8]). *Consider LBB-stable conforming FE pairs such that $Q_h \subset H^1(\Omega)$, then the following condition holds*

$$\inf_{p_h\in Q_h}\sup_{\mathbf{u}_h\in\mathbf{V}_h}\frac{(\operatorname{div}\mathbf{u}_h,\, p_h)}{\|\nabla p_h\|\,\|\mathbf{u}_h\|} \geqslant \beta_1 > 0, \tag{27}$$

where β_1 is independent of h.

Proof. Given in the Appendix. □

Remark. Lemma 4.1 is applicable to the family of Taylor–Hood P_{k+1}/P_k pairs with $k\geqslant 1$. For the particular case of $k=1$ the result can be found in [2]. Analysing the reduced SUPG method we found it more convenient to use the condition (27), rather than (6).

The stability result is given in the following lemma. We set $\sigma_b = \sigma_0 h^2$.

Lemma 4.2. *Assume such scaling of* (2) *that* $\|\mathbf{a}\|_\infty \sim 1$. *Let the following parameter conditions be valid*:

$$\delta_\tau \mathbf{a}_\tau^2 \leqslant \gamma_\tau \leqslant \gamma; \quad 0 \leqslant \delta_\tau = \delta_0 h_\tau^2 \leqslant \min\left\{ \frac{\nu + \alpha h_\tau^2 \mu_u^{-2}}{8\mathbf{a}_\tau^2}; \frac{h_\tau^2}{3\mu_u^2 \nu}; \frac{1}{3\alpha} \right\} \tag{28}$$

with $\gamma = \mathrm{O}(1)$, $\mathbf{a}_\tau := \|\mathbf{a}\|_{\infty,\tau}$. *Then there exist positive constants* $\beta_b \neq \beta_b(h, \nu)$ *and* σ_b *such that*

$$\inf_{U_h \in \mathbf{W}_h} \sup_{V_h \in \mathbf{W}_h} \frac{a_h(U_h, V_h)}{|||U_h|||_b |||V_h|||_b} \geqslant \beta_b. \tag{29}$$

The scheme (7)–(9) *with* (23) *has a unique solution* $U_h = (\mathbf{u}_h, p_h) \in \mathbf{W}_h$.

Proof. Given in the Appendix. □

The main restriction on the SUPG parameter δ_τ is hidden in (28):

$$\delta_\tau = \delta_0 h_\tau^2 \leqslant \frac{\nu + \alpha h_\tau^2 \mu_u^{-2}}{8\mathbf{a}_\tau^2}. \tag{30}$$

The condition (30) is fulfilled for moderate up to large values of α. This allows small up to moderate time steps in a transient approach to the nonlinear model (1). Considering the worst case in (30) of $\alpha = 0$, we obtain the restriction

$$\mathrm{Re}_\tau := \frac{h_\tau \mathbf{a}_\tau}{\nu} \leqslant \frac{1}{2\sqrt{2\delta_0 \nu}}.$$

Note that the range of "allowed" Re_τ here is significantly larger than for the (unstabilized) Galerkin method, where a satisfactory stability estimate requires $\mathrm{Re}_\tau = \mathrm{O}(1)$. Moreover, we do not see restriction (30) in the numerical experiments presented in Section 5, which show uniform error estimates even for $\alpha = 0$ and $\nu \to 0$. Hence the results of Lemma 4.2 might not be optimal for $\alpha \to 0$. On the other hand the case of $\alpha = 0$ and $\nu \to 0$ might not be of a large physical relevance, since for large Reynolds numbers flows are typically unsteady.

As the next step we obtain the following continuity estimate for a_h.

Lemma 4.3. *For arbitrary* $U = \{\mathbf{u}, p\} \in \mathbf{W}$ *with* $-\nu\Delta\mathbf{u} + \nabla p \in L^2(\tau)^n \ \forall \tau \in \mathscr{T}_h$ *and* $V_h \in \mathbf{W}_h \backslash \{0\}$ *it holds*

$$\begin{aligned} \frac{a_h(U, V_h)}{|||V_h|||_b} \leqslant |[U]|_b + \frac{1}{\sqrt{\sigma_b}} \|\mathbf{u}\| + \left(\sum_\tau \frac{3\mathbf{a}_\tau^2}{\nu + \alpha h_\tau^2 + \mathbf{a}_\tau^2 \delta_\tau} \|\mathbf{u}\|_\tau^2 \right)^{1/2} \\ + \left(\sum_\tau \frac{3}{\nu + \alpha h_\tau^2 + \gamma_\tau} \|p\|_\tau^2 \right)^{1/2} + \left(\sum_\tau \delta_\tau \| - \nu\Delta\mathbf{u} + \alpha\mathbf{u} + \nabla p\|_\tau^2 \right)^{1/2}. \end{aligned} \tag{31}$$

Proof. Follows with the same arguments as the proof of Lemma 3.2. □

The goal is to derive error estimates and the design of the stabilization parameter sets $\{\delta_\tau\}$ and $\{\gamma_\tau\}$. Let $\{\mathbf{u}, p\} \in \mathbf{W}$ and $\{\mathbf{u}_h, p_h\} \in \mathbf{W}_h$ be the solutions of the continuous and of the discrete problems, respectively.

Theorem 4.1. *Suppose that Ω is such that a H^2-regularity result holds for the Stokes problem. Consider LBB-stable FE pairs such that $Q_h \subset H^1(\Omega)$. Assume condition* (26)*, a scaling of equation (2) such that $\|\mathbf{a}\|_\infty \sim 1$ and let the parameters*

$$\gamma_\tau = \gamma \sim 1, \quad \delta_\tau \sim h_\tau^2/\gamma, \quad \sigma_b \sim h^2 \tag{32}$$

satisfy conditions (28)*. Then for the error $E_h = \{\mathbf{u} - \mathbf{u}_h,\, p - p_h\}$ the uniform estimate holds*

$$|||E_h|||_b^2 \leqslant C \sum_\tau (h_\tau^{2(k+1)} |p|^2_{H^{k+1}(\tau)} + h_\tau^{2l} |\mathbf{u}|^2_{H^{l+1}(\tau)}), \quad C \neq C(h, \nu, \alpha). \tag{33}$$

Proof. We follow the lines of the proof of Theorem 3.1, also using the notation introduced there. Using Lemmas 4.2 and 4.3 with $U = \{\eta_\mathbf{u}, \eta_p\}$, we get

$$\begin{aligned}\beta_b |||\{\chi_\mathbf{u}, \chi_p\}|||_b \leqslant |[\{\eta_\mathbf{u}, \eta_p\}]|_b + \frac{1}{\sqrt{\sigma_b}} \|\eta_\mathbf{u}\| + \left(\sum_\tau \delta_\tau \| - \nu \Delta \eta_\mathbf{u} + \alpha \eta_\mathbf{u} + \nabla \eta_p \|_\tau^2 \right)^{1/2} \\ + \left(\sum_\tau \frac{3}{\nu + \alpha h_\tau^2 + \gamma_\tau} \|\eta_p\|_\tau^2 \right)^{1/2} + \left(\sum_\tau \frac{3\mathbf{a}_\tau^2}{\nu + \alpha h_\tau^2 + \mathbf{a}_\tau^2 \delta_\tau} \|\eta_\mathbf{u}\|_\tau^2 \right)^{1/2}.\end{aligned}$$

The triangle inequality $|||E_h|||_b \leqslant |||\{\chi_\mathbf{u}, \chi_p\}|||_b + |||\{\eta_\mathbf{u}, \eta_p\}|||_b$ and the standard interpolation properties, together with the assumptions $\nu \delta_\tau \leqslant C h_\tau^2$ and $\alpha \delta_\tau \leqslant C$ from (28), imply that

$$\begin{aligned}|||E_h|||_b^2 \leqslant C \sum_\tau \left\{ \left(\delta_\tau + \sigma_b + \frac{h_\tau^2}{\nu + \alpha h_\tau^2 + \gamma_\tau} \right) h_\tau^{2k} |p|^2_{H^{k+1}(\tau)} \right. \\ \left. + \left(\nu + \alpha h_\tau^2 + \gamma_\tau + \frac{h_\tau^2}{\sigma_b} + \delta_\tau \mathbf{a}_\tau^2 + \frac{\mathbf{a}_\tau^2}{\nu + \alpha h_\tau^2 + \mathbf{a}_\tau^2 \delta_\tau} h_\tau^2 \right) h_\tau^{2l} |\mathbf{u}|^2_{H^{l+1}(\tau)} \right\}.\end{aligned} \tag{34}$$

Recalling the usual condition $l \geqslant k + 1$ for LBB-stable pairs, the estimate (34), together with the design conditions (32) imply the desired result. □

Remark. Another possible or further reduction of stabilization terms give rise to "classical" SUPG-stabilization ($\delta_\tau > 0$, $\gamma_\tau = 0$) or grad-div stabilization ($\delta_\tau = 0$, $\gamma_\tau > 0$). It is not our intention here to study these schemes in detail. We remark that the Lemmas 3.1 or 4.2 are not applicable for the case $\gamma_\tau = 0$. If $\delta_\tau = 0$ the stability result of Lemma 3.1 remains valid, whereas Lemma 3.2 requires minor modifications.

Summarizing some properties of the reduced schemes, we note the following.

- The assembling process of the discrete systems is cheaper than for the fully stabilized schemes considered in Section 3.
- The existing analysis of the scheme shows explicit control of the classical SUPG velocity error

$$\sum_\tau h_\tau^2 \|(\mathbf{a} \cdot \nabla)\mathbf{e}_u\|_\tau^2 \leqslant C \sum_\tau (h_\tau^{2(k+1)} |p|^2_{H^{k+1}(\tau)} + h_\tau^{2l} |\mathbf{u}|^2_{H^{l+1}(\tau)}).$$

We were not able to show this result for the fully stabilized schemes.

- The obtained stability estimates are not completely satisfactory yet, however they are significantly better than for the unstabilized Galerkin method.

5. Numerical results for the Oseen problem

Here we apply the package $FEMLAB^{TM}$ 2.3 which contains the P_{k+1}/P_k pairs of the Taylor–Hood family with $k \geqslant 1$ on simplicial meshes. $FEMLAB^{TM}$ provides SUPG-stabilization in the sense of Section 3 with parameters δ_τ close to (22) but without grad-div stabilization, i.e. $\gamma_\tau = 0$. Therefore we added MATLAB routines with different stabilization terms. Here we present some numerical experiments for the linearized problem (2).

We consider two examples on an unstructured quasi-uniform triangular mesh in the unit square $\Omega = (0, 1) \times (0, 1)$. The right-hand sides $\mathbf{f}$ and the Dirichlet data of problem (2) are chosen such that the exact solutions are given by

$$\text{P1:}\ \ \mathbf{u}(x) = (\sin(\pi x_1), -\pi x_2 \cos(\pi x_1))^T, \quad p(x) = \sin(\pi x_1)\cos(\pi x_2)$$

$$\text{P2:}\ \ \mathbf{u}(x) = (1 - h(x_2, \nu), 0)^T, \quad p(x) = \sqrt{\nu} x_1 h(x_2, \nu)$$

with $h(x_2, \nu) := \exp\frac{-x_2}{\sqrt{\nu}} + \exp\frac{-(1-x_2)}{\sqrt{\nu}}$. We set $\mathbf{a}(x) := \mathbf{u}(x)$ and $\alpha = 0$.

Note that the solution P1 is ν-independent, whereas the ν-dependent solution P2 mimics a "plug-flow" in a channel with exponential layers for $0 < \nu \ll 1$. The seminorms of the solution of P2 appearing on the right-hand side of the error estimates are ν-dependent as $|\mathbf{u}|_{l+1} \sim \nu^{-1/2(l+1/2)}$, $|p|_{k+1} \sim \nu^{-1/2(k-1/2)}$.

Experiment 5.1. Theoretical vs. numerical order for the full norm.

For the fully stabilized scheme we compare the numerical results for problem P1 to the error estimate w.r.t. the full norm $|||\cdot|||_a$ as predicted by Theorem 3.1. (For results for problem P2 see Experiment 5.3.) Here we consider the viscosities $\nu = 10^{-2i}$, $i \in \{1, 2, 3, 4\}$. Results are given for the P_2/P_1 and P_4/P_3 elements.

We start with the stabilization parameters according to Theorem 3.1. The results for the ν-independent solution of P1 in Fig. 1 (left) confirm both, the robustness w.r.t. ν and the predicted error order, of the scheme. Moreover, one observes the considerable improvement with higher order elements. It is worthwhile commenting that the P_2/P_1 element gives much better results than the stabilized P_1/P_1 pair and compares well to P_2/P_2.

Then we compare the new parameter design conditions (17), cf. Theorem 3.1, to the standard equal-order design (22). In Fig. 1 (right) we present the results for the equal-order design (22) w.r.t. the norm $|||\cdot|||_a$ for problem P1. We observe the predicted order reduction of $\frac{1}{2}$. For other norms we refer to Experiment 5.2.

Finally we compared the theoretical error estimates for the reduced stabilized scheme, cf. Theorem 4.1, w.r.t. $|||\cdot|||_b$ to the numerical results for P1. We omit the results here since there is no visible difference to the results for the fully stabilized scheme.

Experiment 5.2. Fully stabilized vs. reduced stabilized scheme.

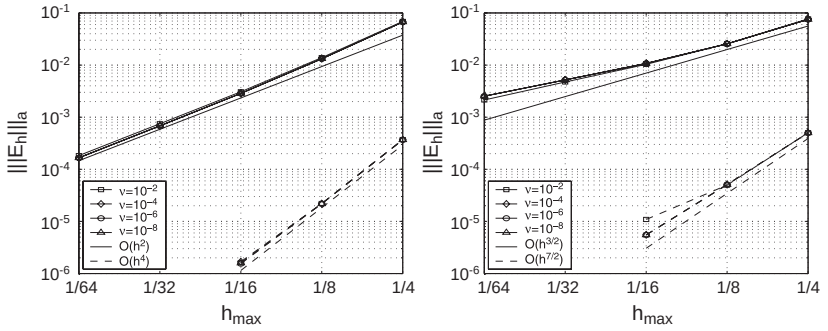

Fig. 1. Fully stabilized scheme for PI. Left: New parameter design P_2/P_1 (full line), P_4/P_3 (broken line). Right: Equal-order parameter design P_2/P_1 (full line), P_4/P_3 (broken line).

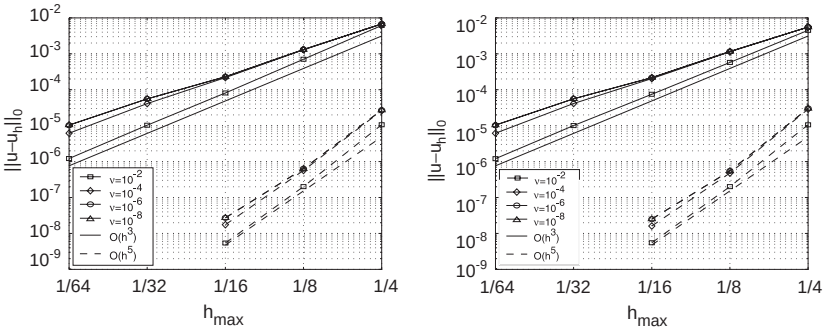

Fig. 2. Fully (left) and reduced (right) stabilized schemes for P1 with P_2/P_1 (full line) and P_4/P_3 (broken line) schemes: Convergence of $\|\mathbf{u} - \mathbf{u}_h\|_0$.

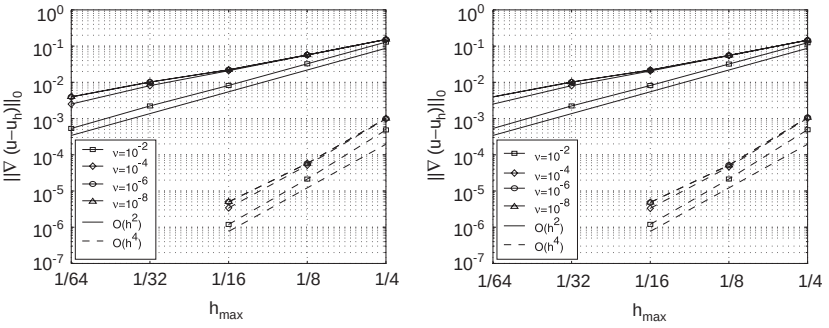

Fig. 3. Fully (left) and reduced (right) stabilized schemes for P1 with P_2/P_1 (full line) and P_4/P_3 (broken line) schemes: Convergence of $\|\nabla(\mathbf{u} - \mathbf{u}_h)\|_0$.

For the fully and reduced stabilized schemes and problem P1 we consider the convergence w.r.t. $\|\mathbf{u} - \mathbf{u}_h\|_0$, $|\mathbf{u} - \mathbf{u}_h|_1$, $\|p - p_h\|_0$. In Figs. 2–4 we report the results for the P_2/P_1 and P_4/P_3 pairs, respectively, and the viscosities $\nu = 10^{-2i}$, $i \in \{1, 2, 3, 4\}$. Furthermore we use the design (32).

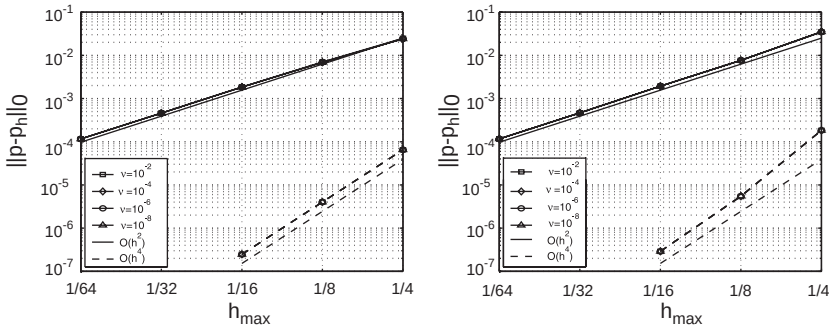

Fig. 4. Fully (left) and reduced (right) stabilized schemes for P1 with P_2/P_1 (full line) and P_4/P_3 (broken line) schemes: Convergence of $\|p - p_h\|_0$.

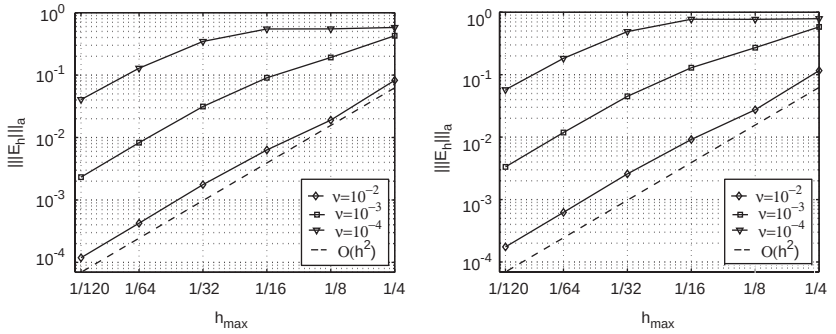

Fig. 5. Fully stabilized (left) and reduced stabilized (right) scheme with new parameter design with P_2/P_1 for P2.

First of all, we see that the results for both schemes are almost the same with the exception of very rough meshes. More precisely, the results for $|\mathbf{u} - \mathbf{u}_h|_1$ and $\|p - p_h\|_0$ are in agreement with the theory of Sections 3–4. Notice that the analysis did not predict the optimal order h^{k+1} for $\|\mathbf{u} - \mathbf{u}_h\|_0$ which is seen in Fig. 2. Moreover, we observe convergence results for $\|\mathrm{div}(\mathbf{u} - \mathbf{u}_h)\|_0$ of, at least, order h^k.

Furthermore, we repeated the computations with the equal-order parameter design (22). We observed (as in Experiment 5.1) the order reduction of $\frac{1}{2}$ for the velocity norms considered here.

The results confirm our conjecture that the PSPG terms can be omitted.

Experiment 5.3. Resolution of boundary layers for P2

For the ν-dependent solution of P2, the predicted rates can be seen for sufficiently fine meshes with $h \leqslant c\sqrt{\nu}$ only. Theorem 3.1 predicts for the P_{k+1}/P_k pair that $|||E_h|||_a \leqslant C\nu^{-\frac{1}{4}}(h\nu^{-\frac{1}{2}})^{k+1}$. On the other hand, the error $|||E_h|||_a$ remains uniformly bounded w.r.t. ν, see Fig. 5 (left). Moreover, we observe as for problem P1 that the reduced scheme gives almost identical results, see Fig. 5 (right). Based on these results, we consider the fully stabilized scheme with parameter design (17).

More interesting is a closer look at the pointwise convergence. In Fig. 6 we present cross-sections of the first velocity component $u_{h,1}(\frac{1}{2}, x_2)$ with $\nu = 10^{-8}$. The Galerkin scheme exhibits spurious global

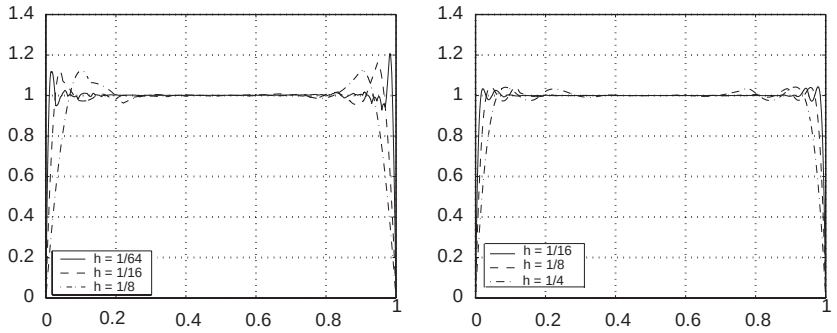

Fig. 6. Fully stabilized scheme for problem P2. Left: P_2/P_1. Right: P_4/P_3.

oscillations (not shown) whereas the stabilized scheme drastically reduces such oscillations. The stabilized scheme generates a solution being well-known from SUPG-stabilization for scalar advection–diffusion problems. The discrete solution is accurate away from the layers but has restricted oscillations around the layer.

As a remarkable and well-known fact we emphasize that the "wiggles" around the layer are significantly reduced with increasing order k. The best way to avoid the wiggles is an anisotropic mesh refinement. Nevertheless the gradient of the solution at the boundary is remarkably sharp. In contrast with problem P1, the SUPG stabilization is much more important than grad-div stabilization.

Experiment 5.4. Influence of $\alpha \sim \frac{1}{\delta t}$ for P1.

So far we considered the Oseen equations with $\alpha = 0$. Here the influence of α for the reduced stabilized scheme is studied. We repeated the computations for problem P1 with $\alpha \in [10^{-3}, 10^{3}]$ and fixed $h_{\max} = \frac{1}{16}$. In order to mimic the effect of a time stepping procedure for the computation of the stationary Navier–Stokes problem we replaced the right-hand side by $\mathbf{f} + \alpha\mathbf{a}$; so the exact solution remains the same. Controlling the norm $|||\cdot|||_b$, we obtain in Fig. 7 robustness from $\alpha \to 0$ up to moderately large values. This result confirms our conjecture that the result of Theorem 4.1 can be extended to $\alpha \to 0$.

Experiment 5.5. Sensitivity w.r.t. tuning parameters for P1.

The stabilized schemes with the parameter choices (17) and (32) depend only on a single "tuning" parameter γ. In Fig. 8 we present the results w.r.t. the norm $|||\cdot|||_a$ for example P1 on a moderate mesh with $h_{\max} = \frac{1}{32}$ using $\gamma_\tau = \gamma = \gamma_0$, $\delta_\tau = h_\tau^2/\gamma_0$ with varying γ_0 and order k of the Taylor–Hood pairs. The robustness of the new parameter design (17) is confirmed. Moreover, we found the choice $\gamma \sim k$ to be an appropriate one.

6. Numerical results for the nonlinear case

In this section we demonstrate the feasibility of the approach to the Navier–Stokes model (1) as proposed in Section 2. The solutions of the benchmark problems are ν-dependent. We apply the semi-implicit Euler

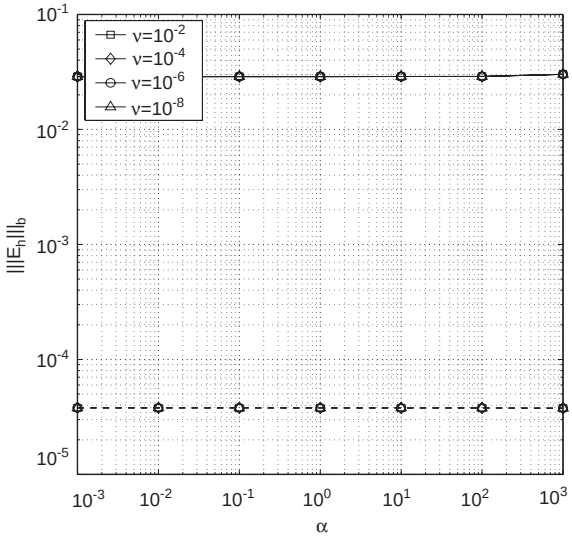

Fig. 7. Influence of α for P1 with reduced scheme. P_2/P_1 (full line), P_4/P_3 (broken line).

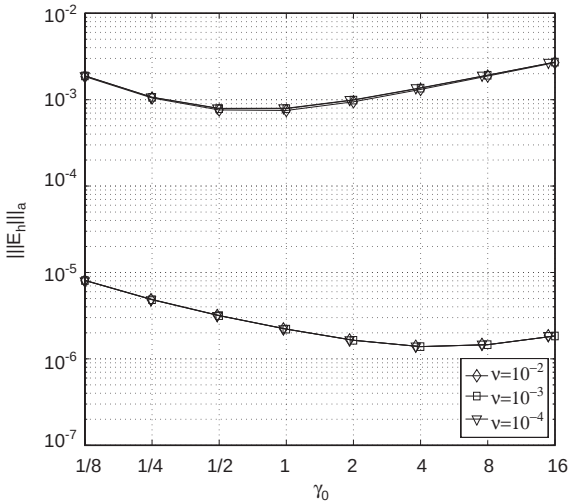

Fig. 8. Influence of γ_0 for P1 with full scheme. P_2/P_1 (top), P_4/P_3 (bottom).

scheme for the time discretization. Then the stabilized schemes of Sections 3–4 are used to solve the auxiliary Oseen problems within each time step.

Example 6.1. (Driven cavity).

Consider problem (1) in the domain $\Omega = (0, 1)^2$, with $\mathbf{f} = (0, 0)^{\mathrm{T}}$ and Dirichlet data $\mathbf{u}|_{\partial\Omega} = (1, 0)^{\mathrm{T}}$ if $x_2 = 1$ and $\mathbf{u}|_{\partial\Omega} = (0, 0)^{\mathrm{T}}$ if $x_2 < 1$. We use a time step $\delta t = 0.1$ and a spatial discretization using

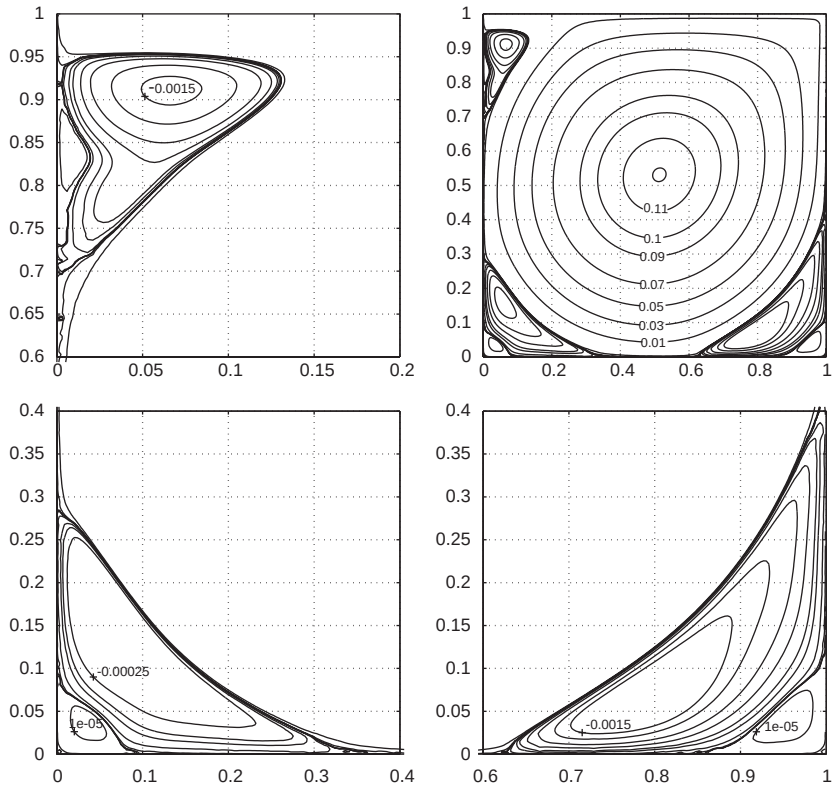

Fig. 9. Isolines of the stream-function for the driven cavity problem for Re = 7.500 with the reduced stabilized scheme: full flow (upper right) and details of the recirculation zones.

the Taylor–Hood elements P_2/P_1 and P_4/P_3 on a quasi-uniform mesh with $h_{\max} = \frac{1}{96}$ and $h_{\max} = \frac{1}{32}$, respectively.

We compared our results for Re $\in \{100, 400, 1.000, 3.200, 7.500, 10.000\}$ with those given in [13] for lower order finite difference schemes but on much finer meshes up to $h = \frac{1}{256}$. The results are comparable, for details cf. [12]. Moreover, we see a nice resolution of the boundary layers which are less sharp as in Problem P2 in Section 5.

As an example, we present results with the reduced stabilized schemes for Re = 7.500 which is below the first Hopf bifurcation for Re $\approx$ 8.018, cf. [1] . The isolines of the stream-function for the full flow together with details of the secondary and tertiary recirculation zones in the corners are shown in Fig. 9 for $h = \frac{1}{48}$. In Table 1 we give the position of the center of the primary vortex of the cavity flow together with the value of the stream function. In Table 2 we give the position and values of the minimum of $u_1(0.5, x_2)$ and of the minimum and maximum of $u_2(x_1, 0.5)$. First of all, we observe a good agreement of the results on moderately fine meshes with the reference solutions of [4,13,18] on much finer grids. Moreover, we see that the results for the fully stabilized and the reduced scheme are very close.

Table 1
Driven cavity problem with Re = 7.500: Position and stream function of main vortex

Reference	Method	Ψ	x_1	x_2
$(a)_1$ Fully stab. scheme	FE P_2/P_1, $h_{\max} = 1/96$	0.1177	0.5129	0.5337
$(a)_2$ Reduced scheme	FE P_2/P_1, $h_{\max} = 1/96$	0.1176	0.5129	0.5337
(b) Red. stab. scheme	FE P_4/P_3, $h_{\max} = 1/32$	0.1151	0.5166	0.5310
(c) Ref. [18]	FD, $h = 1/512$	0.1153	0.5137	0.5321
(d) Ref. [13]	FD, $h = 1/256$	0.1200	0.5117	0.5322

Table 2
Driven cavity problem with Re = 7.500: Minimum value of $u_1(0.5, x_2)$ and minimum and maximum values of $u_2(x_1, 0.5)$

Reference/method	$u_1^{\min}$	$x_2^{\min}$	$u_2^{\max}$	$x_1^{\max}$	$u_2^{\min}$	$x_1^{\min}$
$(a)_1$ Fully stab. P_2/P_1, $h = 1/96$	−0.4322	0.0620	0.4343	0.0685	−0.5535	0.9638
$(a)_2$ Reduced P_2/P_1, $h = 1/96$	−0.4322	0.0620	0.4343	0.0685	−0.5535	0.9638
(b) Reduced P_4/P_3, $h = 1/32$	−0.4213	0.0628	0.4225	0.0694	−0.5396	0.9639
(c) Ref. [4] FD, $h = 1/512$	−0.4266	0.0625	0.4274	0.0684	−0.5455	0.9648
(d) Ref. [13] FD, $h = 1/256$	−0.4359	0.0625	0.4403	0.0703	−0.5522	0.9609

Example 6.2. (Backward facing step).

Finally we consider the two-dimensional flow in a channel with a backward facing step, see [19]. We employed the $h : H = 1 : 2$ configuration (where H is the height of the channel and h the height of the step) with parabolic velocity profile at the inlet. At the outlet we prescribe the usual "do-nothing" condition for the stress tensor. For the remaining boundary of the channel we prescribe no-slip. The flow corresponds to Re = 800.

We apply P_2/P_1 Taylor–Hood elements on an unstructured quasi-uniform mesh with $h_{\max} = 1/32$ and a time step $\delta t = 0.4$ in the interval $0 \leqslant t \leqslant T = 200$. In Fig. 10 one finds the isolines of the stream function and of the pressure of the stationary solution at $t = 200$ for the reduced stabilized scheme with $h = 1/16$. The fully stabilized scheme (not shown) gives almost the same picture. Moreover we compare in Table 3 the results for some critical Re-dependent parameters of the flow with reference values found in literature. The results for the fully stabilized and the reduced schemes are again identical and in very good agreement with reference solutions: an FD solution with $h = 1/40$ in [11], an FD solution on a refined mesh with about 280.000 nodes and Richardson extrapolation in [18] and a spectral element method in [14].

7. Conclusions

Mixed problems of Oseen type appear as auxiliary problems within the solution of the Navier–Stokes problem. The application of conforming LBB-stable FE spaces requires a stabilization in case of large

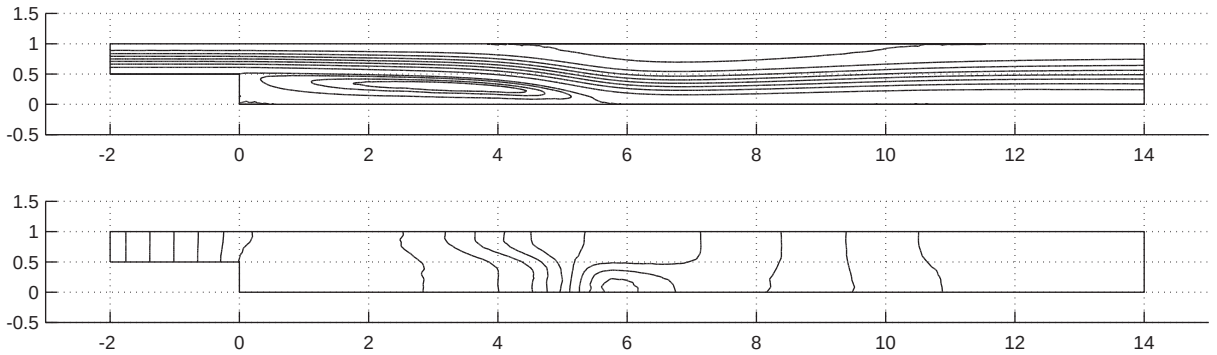

Fig. 10. Isolines of stream function and pressure for backward facing step problem with Re = 800: reduced stabilized scheme with $h = 1/16$.

Table 3
Numerical results for the backward facing step problem with Re = 800. (x_c, y_c)-position of the bottom vortex center, r_1-reattachment length of the bottom vortex, r_2-left separation point of the upper vortex, r_3-right separation point of the upper vortex

Reference	Method	(x_c, y_c)	r_1	r_2	r_3
Fully stab.	FE P_2/P_1, $h_{\max} = 1/32$	(3.40, 0.30)	6.10	4.86	10.48
Reduced stab.	FE P_2/P_1, $h_{\max} = 1/32$	(3.40, 0.30)	6.10	4.86	10.48
Ref. [11]	FD, $h_{\max} = 1/40$	(3.35, 0.30)	6.10	4.85	10.48
Ref. [18]	FD, Extrapol.	(3.40, 0.30)	6.09	4.82	10.47
Ref. [14]	Spectr. element	(3.39, 0.31)	6.10	4.85	10.48

Reynolds numbers Re. Stability without sacrificing accuracy can be reached by SUPG stabilization with and without pressure stabilization (PSPG) however with the grad-div stabilization.

The design of the stabilization parameters is simpler (and in practice less sensitive) for LBB-stable elements than for equal order interpolation. For the fully stabilized scheme studied in Section 3 the proposed choice leads (for smooth Re-independent solutions) to error estimates being robust w.r.t. to Re and quasi-optimal for fixed Re. The parameter design known from equal-order interpolation leads to suboptimal convergence. Numerical experiments confirm the theoretical results for smooth Re-independent solutions; reasonable results were obtained also for Re-dependent solutions.

An open problem is whether PSPG can be omitted for LBB-stable elements. Such a reduced stabilized scheme gives numerical results being almost identical to the fully stabilized scheme. In the paper a previous stability result of this scheme is improved. The numerical results make us to believe that the analysis can be improved even for arbitrary small values of $\alpha \geqslant 0$ and $\nu > 0$.

The approach considered remains feasible for calculation of steady-state solutions of the Navier–Stokes model for moderate and high Re-numbers. The construction of consistent higher-order time discretization, combined with stabilized FE methods, for the nonstationary problem and the development of efficient solvers is left to future research. Another important open question is the extension of the theory to anisotropically refined meshes in boundary layers.

Appendix. Proof of stability results

Proof of Lemma 3.1. Fix an arbitrary $U_h \in \mathbf{W}_h$. Below we find $V_h \in \mathbf{W}_h$ satisfying (14). We use the following abbreviations:

$$A^2 := \nu\|\nabla \mathbf{u}_h\|^2 + \alpha\|\mathbf{u}_h\|^2, \quad B^2 := \|p_h\|^2, \quad Z^2 := \sum_\tau \gamma_\tau \|\operatorname{div} \mathbf{u}_h\|_\tau^2,$$

$$X^2 := \sum_\tau \delta_\tau \|(\mathbf{a}\cdot\nabla)\mathbf{u}_h + \nabla p_h\|_\tau^2, \quad Y^2 := \sum_\tau \delta_\tau \|-\nu\Delta \mathbf{u}_h + \alpha \mathbf{u}_h\|_\tau^2,$$

hence $|[U_h]|_a^2 = A^2 + X^2 + Z^2$. In the first step we set $V_h = U_h$ in (8), thus

$$a_h(U_h, U_h) \geqslant A^2 + X^2 + Z^2 - XY.$$

We get from inverse inequalities and (13) that $Y \leqslant A$; then Young's inequality implies

$$a_h(U_h, U_h) \geqslant \frac{1}{2}(A^2 + X^2 + Z^2). \tag{35}$$

Condition (6) yields the existence of $\mathbf{z}_h \in \mathbf{V}_h$ with $(\operatorname{div} \mathbf{z}_h,\ p_h) \geqslant \beta_0 \|p_h\|_Q \|\mathbf{z}_h\|_{\mathbf{V}}$. We can assume $\|\mathbf{z}_h\|_{\mathbf{V}} = \|p_h\|_Q$. Consider now

$$a_h(U_h, (\mathbf{z}_h, 0)) = (p_h, \operatorname{div} \mathbf{z}_h) - \sum_{i=1}^4 T_i \geqslant \beta_1 B^2 - \sum_{i=1}^4 T_i.$$

Denote $\gamma = \max_\tau \gamma_\tau$. Standard inequalities, integration of the advective term by parts, and (13) imply

$$\begin{aligned} T_1 &= \nu(\nabla \mathbf{u}_h, \nabla \mathbf{z}_h) + (\alpha \mathbf{u}_h, \mathbf{z}_h) - (\mathbf{u}_h, (\mathbf{a}\cdot\nabla)\mathbf{z}_h) \\ &\leqslant \left(\sqrt{\nu} + \sqrt{\alpha} C_F^2 + \frac{C_F \|\mathbf{a}\|_\infty}{\sqrt{\nu + \alpha C_F^2}}\right) AB, \end{aligned}$$

$$T_2 = \sum_\tau \gamma_\tau (\operatorname{div} \mathbf{u}_h, \operatorname{div} \mathbf{z}_h)_\tau \leqslant \sqrt{\gamma} ZB,$$

$$T_3 = \sum_\tau \delta_\tau (-\nu\Delta \mathbf{u}_h + \alpha \mathbf{u}_h, (\mathbf{a}\cdot\nabla)\mathbf{z}_h)_\tau \leqslant \max_\tau (\sqrt{\delta_\tau}\mathbf{a}_\tau) AB \leqslant \sqrt{\gamma} AB,$$

$$T_4 = \sum_\tau \delta_\tau ((\mathbf{a}\cdot\nabla)\mathbf{u}_h + \nabla p_h, \mathbf{a}\cdot\nabla \mathbf{z}_h)_\tau \leqslant \max_\tau (\sqrt{\delta_\tau}\mathbf{a}_\tau) XB \leqslant \sqrt{\gamma} XB.$$

We set $\zeta_a := \sqrt{\nu} + \sqrt{\alpha} C_F^2 + \frac{C_F \|\mathbf{a}\|_\infty}{\sqrt{\nu + \alpha C_F^2}} + \sqrt{\gamma}$ and use Young's inequality; hence

$$a_h(U_h, (-\mathbf{z}_h, 0)) \geqslant \beta_0^2 - \zeta_a (A + X + Z)B \geqslant \frac{1}{2}\beta_0 B^2 - \frac{3\zeta_a^2}{\beta_0}(A^2 + X^2 + Z^2). \tag{36}$$

Setting $V_h := U_h + \rho_a(-\mathbf{z}_h, 0)$ with $\rho_a = \frac{\beta_0}{12\zeta_a^2}$, $\sigma_a := 2\beta_0\rho_a$, we find by (35), (36)

$$a_h(U_h, V_h) \geqslant \min\left(\frac{1}{2} - \frac{3\rho_a\zeta_a^2}{\beta_0}; \frac{\beta_0\rho_a}{2\sigma_a}\right)(|[U]|_a^2 + \sigma_a B^2) \geqslant \frac{1}{4}|||U_h|||_a^2. \tag{37}$$

Furthermore, we obtain with (13)

$$\begin{aligned}|||(-\mathbf{z}_h, 0)|||_a^2 &= \nu\|\nabla\mathbf{z}_h\|^2 + \alpha\|\mathbf{z}_h\|^2 + \sum_\tau(\delta_\tau\|\mathbf{a}\cdot\nabla\mathbf{z}_h\|_\tau^2 + \gamma_\tau\|\operatorname{div}\mathbf{z}_h\|_\tau^2)\\ &\leqslant (\nu + \alpha C_F^2 + 2\gamma)\|\nabla\mathbf{z}_h\|^2 \leqslant 2\zeta_a^2 B^2.\end{aligned}$$

By definition of ρ_a and σ_a we have $6\rho_a^2\zeta_a^2 \leqslant \frac{1}{12}\sigma_a$; hence

$$|||V_h|||_a^2 \leqslant 2(|||U_h|||_a^2 + \rho_a^2|||(-\mathbf{z}_h, 0)|||_a^2) \leqslant \frac{13}{6}|||U_h|||_a^2,$$

which together with (37) implies (14) with $\beta_a = \frac{1}{4}\sqrt{\frac{6}{13}}$. Finally we note that parameter σ_a can be set as given in (15). The lemma is proved. □

Proof of Lemma 4.1. Denote by $S_h(\varepsilon) : Q_h \to Q_h$ an operator defined as $S_h(\varepsilon) = BA(\varepsilon)^{-1}B^*$, where operators $A(\varepsilon) : \mathbf{V}_h \to \mathbf{V}_h$ and $B : \mathbf{V}_h \to Q_h$ are defined by the relations

$$(A(\varepsilon)\mathbf{u}_h, \mathbf{v}_h) = \varepsilon(\nabla\mathbf{u}_h, \nabla\mathbf{v}_h) + (\mathbf{u}_h, \mathbf{v}_h) \quad \forall\mathbf{u}_h, \mathbf{v}_h \in \mathbf{V}_h,$$

$$(B\mathbf{u}_h, q_h) = (\operatorname{div}\mathbf{u}_h, q_h) \quad \forall\mathbf{u}_h \in \mathbf{V}_h,\ q_h \in Q_h.$$

Let Δ_h^{-1} be a solution operator for the discrete Poisson problem with the Neumann boundary conditions: for any $q_h \in Q_h$

$$r_h = \Delta_h^{-1}q_h \quad \text{iff} \quad -(\nabla r_h, \nabla\xi) = (q_h, \xi) \quad \forall\xi \in Q_h. \tag{38}$$

The corollary 4.1 from [3] supplies us with the estimate

$$c_0((h^2 I - \Delta_h^{-1})^{-1}p_h, p_h) \leqslant (S_h(h^2)p_h, p_h) \quad \forall p_h \in Q_h. \tag{39}$$

c_0 is a positive constant independent of h, I is the identity operator. It is straightforward to check for arbitrary $p_h \in Q_h$

$$\begin{aligned}(S_h(h^2)p_h, p_h) &= \sup_{\mathbf{u}_h\in\mathbf{V}_h}\frac{(p_h, B\mathbf{u}_h)^2}{(A(h^2)\mathbf{u}_h, \mathbf{u}_h)} = \sup_{\mathbf{u}_h\in\mathbf{V}_h}\frac{(\operatorname{div}\mathbf{u}_h, p_h)^2}{h^2\|\nabla\mathbf{u}_h\|^2 + \|\mathbf{u}_h\|^2}\\ &\leqslant \sup_{\mathbf{u}_h\in\mathbf{V}_h}\frac{(\operatorname{div}\mathbf{u}_h, p_h)^2}{\|\mathbf{u}_h\|^2}.\end{aligned} \tag{40}$$

On the other hand (27) is equivalent to the inequality

$$\beta_1\|\nabla p_h\| \leqslant \sup_{\mathbf{u}_h\in\mathbf{V}_h}\frac{(\operatorname{div}\mathbf{u}_h, p_h)}{\|\mathbf{u}_h\|} \quad \forall p_h \in Q_h.$$

Therefore, thanks to (39) and (40) it is sufficient to prove that

$$c_1\|\nabla p_h\|^2 \leqslant ((h^2 I - \Delta_h^{-1})^{-1} p_h, p_h) \quad \forall p_h \in Q_h \tag{41}$$

with some $c_1 > 0$ independent of h. To prove (41) let us fix arbitrary $p_h \in Q_h$ and denote $q_h = (h^2 I - \Delta_h^{-1})^{-1} p_h$, then by definition

$$h^2 q_h - \Delta_h^{-1} q_h = p_h. \tag{42}$$

Let $r_h = \Delta_h^{-1} q_h$, yielding $r_h = h^2 q_h - p_h$. Substituting this into (38) and choosing $\xi = p_h$, we get

$$-h^2(\nabla q_h, \nabla p_h) + \|\nabla p_h\|^2 = (q_h, p_h).$$

This implies

$$(q_h, p_h) \geqslant \frac{1}{2}\|\nabla p_h\|^2 - \frac{1}{2} h^4 \|\nabla q_h\|^2. \tag{43}$$

Now we take a scalar product of (42) and q_h to get

$$(p_h, q_h) = h^2\|q_h\|^2 + \|q_h\|_{-1}^2 \geqslant h^2\|q_h\|^2.$$

Due to the inverse inequality (4) this leads to

$$(p_h, q_h) \geqslant \mu_p^{-1} h^4 \|\nabla q_h\|^2. \tag{44}$$

We combine (43) and (44) to obtain

$$(p_h, q_h) \geqslant (2 + \mu_p)^{-1} \|\nabla p_h\|^2.$$

The latter estimate implies (41) with $c_1 = (2 + \mu_p)^{-1}$. □

Proof of Lemma 4.2. The proof follows the lines of that of Lemma 3.1; so we highlight the modifications. We use the following modified abbreviations:

$$\tilde{X}^2 := \sum_\tau \delta_\tau \|(\mathbf{a}\cdot\nabla)\mathbf{u}_h\|_\tau^2, \quad \tilde{Y}^2 := \sum_\tau \delta_\tau \| - \nu\Delta\mathbf{u}_h + \alpha\mathbf{u}_h + \nabla p_h\|_\tau^2,$$

and $\tilde{B}^2 := \|\nabla p_h\|^2$; hence $|[U_h]|_b^2 = A^2 + \tilde{X}^2 + Z^2$. Denote $\delta = \max_\tau \delta_\tau$.

In the first step we set $V_h = U_h$ in (8), thus $a_h(U_h, U_h) \geqslant |[U_h]|_b^2 - \tilde{X}\tilde{Y}$. We have, via triangle inequality, inverse inequalities (4), and using (28),

$$\tilde{Y}^2 \leqslant 3\sum_\tau \delta_\tau(\|\nu\Delta\mathbf{u}_h\|_\tau^2 + \|\alpha\mathbf{u}_h\|_\tau^2 + \|\nabla p_h\|_\tau^2) \leqslant A^2 + 3\delta\tilde{B}^2, \tag{45}$$

hence

$$a_h(U_h, U_h) \geqslant \frac{1}{2}|[U_h]|_b^2 - \frac{3\delta}{2}\tilde{B}^2. \tag{46}$$

Lemma 4.1 implies the existence of $\mathbf{z}_h \in \mathbf{V}_h$ with $(\operatorname{div}\mathbf{z}_h,\, p_h) \geqslant \beta_1 \|\nabla p_h\| \|\mathbf{z}_h\|$ with $\beta_1 \neq \beta_1(h)$. We can assume $\|\mathbf{z}_h\| = \|\nabla p_h\| = \tilde{B}$. Consider now

$$a_h(U_h, (\mathbf{z}_h, 0)) = (p_h, \operatorname{div}\mathbf{z}_h) - \sum_{i=1}^{4} \tilde{T}_i \geqslant \beta_1 \tilde{B}^2 - \sum_{i=1}^{4} \tilde{T}_i.$$

Standard inequalities and condition (28) imply

$$\tilde{T}_1 := T_1 \leqslant \max_\tau \left(\frac{\sqrt{\nu + \alpha h_\tau^2 \mu_u^{-2}}\mu_u\sqrt{2}}{h_\tau} + \frac{\mathbf{a}_\tau\sqrt{2}}{\sqrt{\nu + \alpha h_\tau^2 \mu_u^{-2}}} \right) A\tilde{B}$$

$$\tilde{T}_2 := T_2 \leqslant \max_\tau \frac{\sqrt{\gamma_\tau}\mu_u}{h_\tau}\, Z\tilde{B}$$

$$\begin{aligned}\tilde{T}_3 &:= \sum_\tau \delta_\tau(-\nu\Delta\mathbf{u}_h + \alpha\mathbf{u}_h + \nabla p_h, (\mathbf{a}\cdot\nabla)\mathbf{z}_h)_\tau \leqslant \max_\tau \frac{\sqrt{\delta_\tau}\mathbf{a}_\tau\mu_u}{h_\tau}\, \tilde{Y}\tilde{B} \\ &\leqslant \max_\tau \frac{\sqrt{\gamma_\tau}\mu_u}{h_\tau}\, A\tilde{B} + \max_\tau \frac{\sqrt{3}\delta_\tau\mathbf{a}_\tau\mu_u}{h_\tau}\, \tilde{B}^2 \leqslant \max_\tau \frac{\sqrt{\gamma_\tau}\mu_u}{h_\tau}\, A\tilde{B} + \frac{1}{4}\beta_1\tilde{B}^2,\end{aligned}$$

$$\tilde{T}_4 := \sum_\tau \delta_\tau((\mathbf{a}\cdot\nabla)\mathbf{u}_h, (\mathbf{a}\cdot\nabla)\mathbf{z}_h)_\tau \leqslant \tilde{X} \max_\tau \frac{\sqrt{\delta_\tau}\mathbf{a}_\tau\mu_u}{h_\tau}\, \tilde{B} \leqslant \max_\tau \frac{\sqrt{\gamma_\tau}\mu_u}{h_\tau}\, \tilde{X}\tilde{B}.$$

In the last estimate of $\tilde{T}_3$ we used inequality (45) and a sufficiently small h_τ. We summarize these estimates, set

$$\zeta_b := \max_\tau \left(\frac{\sqrt{\nu + \alpha h_\tau^2 \mu_u^{-2}}\mu_u\sqrt{2}}{h_\tau} + \frac{\mathbf{a}_\tau\sqrt{2}}{\sqrt{\nu + \alpha h_\tau^2 \mu_u^{-2}}} + \sqrt{\gamma_\tau} h_\tau^{-1}\mu_u \right),$$

and use Young's inequality

$$\begin{aligned}a_h(U_h, (-\mathbf{z}_h, 0)) &\geqslant \beta_1\tilde{B}^2 - \zeta_b(A + \tilde{X} + Z)\tilde{B} - \frac{1}{4}\beta_1\tilde{B}^2 \\ &\geqslant \frac{1}{2}\beta_1\tilde{B}^2 - \frac{3}{\beta_1}\zeta_b^2 |[U_h]|_b^2. \end{aligned} \tag{47}$$

Define $V_h := U_h + \rho_b(-\mathbf{z}_h, 0)$ with some $\rho_b > 0$, then via (46), (47)

$$\begin{aligned}a_h(U_h, V_h) &\geqslant \left(\frac{1}{2} - \frac{3\rho_b\zeta_b^2}{\beta_1}\right) |[U_h]|_b^2 + \frac{\beta_1\rho_b - 3\delta}{2}\, \tilde{B}^2 \\ &\geqslant \min\left\{\frac{1}{2} - \frac{3\rho_b\zeta_b^2}{\beta_1};\, \frac{\beta_1\rho_b - 3\delta}{2\sigma_b}\right\} (|[U_h]|_b^2 + \sigma B^2). \end{aligned} \tag{48}$$

We have to find appropriate values of ρ_b and σ_b. (28) implies

$$\zeta_b \leqslant \max_\tau \left(\frac{\sqrt{\nu + \alpha h_\tau^2 \mu_u^{-2}}\mu_u\sqrt{2}}{h_\tau} + \frac{1}{2\sqrt{\delta_\tau}} + \frac{\sqrt{\gamma_\tau}\mu_u}{h_\tau} \right) \leqslant \max_\tau \frac{c}{h_\tau}, \tag{49}$$

where we use that $\delta = \delta_0 h_\tau^2$. Fixing $\rho_b \zeta_b^2 = \frac{\beta_1}{12}$, we obtain on a quasi-uniform mesh that

$$\beta_1\rho_b - 3\delta = \frac{\beta_1^2}{12\zeta_b^2} - 3\delta \geqslant \frac{\beta_1^2 h_{\min}^2}{12c^2} - 3\delta_0 h_{\max}^2 \geqslant \left(\frac{\beta_1 c_1}{12c^2} - 3\delta_0 \right) h^2 =: \tilde{\beta}_1 h^2.$$

A proper choice of δ_0 gives a positive $\tilde{\beta}_1$. Together with $\sigma_b = 2\tilde{\beta}_1 h^2$ we observe

$$a_h(U_h, V_h) \geqslant \frac{1}{4} |||U_h|||_b^2. \tag{50}$$

Furthermore the following estimate holds

$$\begin{aligned} |||(-\mathbf{z}_h, 0)|||_b^2 &= \nu \|\nabla \mathbf{z}_h\|^2 + \alpha \|\mathbf{z}_h\|^2 + \sum_\tau [\delta_\tau \|(\mathbf{a}\cdot\nabla)\mathbf{z}_h\|_\tau^2 + \gamma_\tau \|\operatorname{div} \mathbf{z}_h\|_\tau^2] \\ &\leqslant \max_\tau \left(\frac{\nu\mu_u^2}{h_\tau^2} + \alpha + \max_\tau \left(\frac{\delta_\tau \mathbf{a}_\tau^2 \mu_u^2}{h_\tau^2} + \frac{\gamma_\tau \mu_u^2}{h_\tau^2} \right) \right) \tilde{B}^2 \leqslant \zeta_b^2 \tilde{B}^2. \end{aligned}$$

By the definition of ρ_b we have $\rho_b^2 \zeta_b^2 = \frac{\beta_1}{12}\rho_b$, and hence

$$|||V_h|||_b^2 \leqslant 2|||U_h|||_b^2 + 2\rho_b^2 |||(-\mathbf{z}_h, 0)|||_b^2 \leqslant 2\left(1 + \frac{\beta_1\rho_b}{12\sigma_b}\right) |||U_h|||_b^2.$$

Moreover, we obtain $\beta_1\rho_b = \frac{\beta_1^2}{12\zeta_b^2} \leqslant \frac{\beta_1^2 h^2}{12c^2}$ and

$$1 + \frac{\beta_1\rho_b}{12\sigma_b} \leqslant 1 + \frac{\beta_1^2 h^2}{12c^2 \cdot 2\tilde{\beta}_1 h^2} = 1 + \frac{\beta_1^2}{24c^2\tilde{\beta}_1} =: Q^2.$$

This, together with (50), implies the desired estimate (29) with $\beta = \frac{1}{4\sqrt{2}Q}$. □

References

[1] F. Auteri, N. Parolini, L. Quartapelle, Numerical investigation on the stability of singular driven cavity flow, J. Comput. Phys. 183 (2002) 1–25.
[2] M. Bercovier, O. Pironneau, Error estimates for finite element method solution of the Stokes problem in primitive variables, Numer. Math. 33 (1979) 211–224.
[3] J.H. Bramble, J.E. Pasciak, Iterative techniques for time dependent Stokes problems, Comput. Mathem. Appl. 33 (1997) 13–30.
[4] C. Christov, Personal communication, 2004.
[5] P.G. Ciarlet, Basic error estimates for elliptic problems, in: P.G. Ciarlet, J.L. Lions (Eds.), Handbook of Numerical Analysis, vol. 2, North-Holland, Amsterdam, 1991.

[6] R. Codina, A Finite Element Formulation for Viscous Incompressible Flows, Centro, Internac. Metodos Numer Ing., Politec. Cataluna, Barcelona, 1993.
[7] R. Codina, A stabilized finite element method for generalized stationary incompressible flows, Comput. Meth. Appl. Mech. Engrg. 190 (2001) 2681–2706.
[8] M. Dauge, Stationary Stokes and Navier–Stokes systems on two- or three-dimensional domains with corners. Part I: linearized equations, SIAM J. Math. Anal. 20 (1989) 74–97.
[9] W. Dettmer, D. Peric, An analysis of the time integration algorithms for the finite element solutions of incompressible Navier–Stokes equations based on a stabilised formulation, Comput. Meth. Appl. Mech. Engrg. 192 (2003) 1177–1226.
[10] L.P. Franca, S.L. Frey, Stabilized finite element methods. II. The incompressible Navier–Stokes equations, Comput. Meth. Appl. Mech. Engrg. 99 (1992) 209–233.
[11] D.K. Gartling, A test problem for outflow boundary conditions-flow over the back-facing step, Int. J. Numer. Meth. Fluids 11 (1990) 953–967.
[12] T. Gelhard, Stabilized finite element methods for the Oseen equations (in German), Diploma Thesis, Math. Department, University of Göttingen, NAM, 2003.
[13] U. Ghia, K.N. Ghia, C.T. Shin, High-Re solutions for incompressible flow using the Navier–Stokes equations and a multigrid method, J. Comput. Phys. 48 (1982) 387–411.
[14] J. Keskar, D.A. Lyn, Computation of a laminar backward-facing step at Re = 800 with a spectral domain decomposition method, Intern. J. Comput. Fluid Dynam. 29 (1999) 411–427.
[15] P. Knobloch, L. Tobiska, A streamline diffusion method for nonconforming finite element approximations applied to the linearized incompressible Navier–Stokes equations, in: O.P. Iliev et al. (Eds.), Proceedings of the 4th International Conference on Numerical Meths. Applic., Sofia, World Scientific, Singapore, 1999, pp. 530–538.
[16] D. Loghin, Analysis of preconditioned Picard iterations for the Navier–Stokes equations, Oxford University Computer Laboratory, Report no. 01/10, 2001.
[17] G. Lube, M.A. Olshanskii, Stable finite-element calculation of incompressible flows using the rotation form of convection, IMA Journal Numer. Anal. 22 (2002) 437–461.
[18] R.S. Marinova, C.I. Christov, T.T. Marinov, A fully coupled solver for incompressible Navier–Stokes equations using operator splitting, Intern. Journal Comput. Fluid Dynam. 17 (5) (2003) 371–385.
[19] M.A. Olshanskii, A low order Galerkin finite element method for the Navier–Stokes equations of steady incompressible flow: a stabilization issue and iterative methods, Comput. Meth. Appl. Mech. Eng. 141 (2002) 5515–5536.
[20] H.G. Roos, M. Stynes, L. Tobiska, Numerical methods for singularly perturbed differential equations: convection diffusion and flow problems, Springer, Berlin, 1996.
[21] M. Schäfer, S. Turek, Benchmark computations of laminar flow around a cylinder, in: E.H. Hirschel (Ed.), Flow Simulations with High-Performance Computers II, Notes Numer. Fluid Mech. vol. 2, 1996.
[22] L. Tobiska, R. Verfürth, Analysis of a streamline diffusion finite element method for the Stokes and Navier–Stokes equations, SIAM J. Numer. Anal. 33 (1996) 107–127.
[23] S. Turek, Efficient Solvers for Incompressible Flow Problems: An Algorithmic Approach in View of Computational Aspects, Springer, Berlin, 1999.